



## OPEN ACCESS

## EDITED BY

Mohd Saeed,  
University of Hail, Saudi Arabia

## REVIEWED BY

Marcelo Muñoz,  
Facultad de Ciencias, Universidad  
Austral de Chile, Chile  
Rosa E. Del Río,  
Michoacana University of San Nicolás de  
Hidalgo, Mexico

## \*CORRESPONDENCE

Kung-Ta Lee,  
ktleee@ntu.edu.tw  
Yao-Haur Kuo,  
kuoyh@nrcm.edu.tw  
Chia-Ching Liaw,  
liawcc@nrcm.edu.tw

<sup>†</sup>These authors contributed equally to  
this work and share the first authorship

## SPECIALTY SECTION

This article was submitted to Medicinal  
and Pharmaceutical Chemistry,  
a section of the journal  
Frontiers in Chemistry

RECEIVED 26 July 2022

ACCEPTED 22 August 2022

PUBLISHED 15 September 2022

## CITATION

Huang H-T, Lo I-W, Liao G-Y, Lin Y-C,  
Shen Y-C, Huang H-C, Li T-L, Lee K-T,  
Kuo Y-H and Liaw C-C (2022), Anti-  
inflammatory sesquiterpene and  
triterpene acids from *Mesona  
procumbens* Hemsley.  
*Front. Chem.* 10:1003356.  
doi: 10.3389/fchem.2022.1003356

## COPYRIGHT

© 2022 Huang, Lo, Liao, Lin, Shen,  
Huang, Li, Lee, Kuo and Liaw. This is an  
open-access article distributed under  
the terms of the [Creative Commons  
Attribution License \(CC BY\)](https://creativecommons.org/licenses/by/4.0/). The use,  
distribution or reproduction in other  
forums is permitted, provided the  
original author(s) and the copyright  
owner(s) are credited and that the  
original publication in this journal is  
cited, in accordance with accepted  
academic practice. No use, distribution  
or reproduction is permitted which does  
not comply with these terms.

# Anti-inflammatory sesquiterpene and triterpene acids from *Mesona procumbens* Hemsley

Hung-Tse Huang<sup>1,2†</sup>, I-Wen Lo<sup>3†</sup>, Geng-You Liao<sup>4</sup>, Yu-Chi Lin<sup>1</sup>,  
Yuh-Chiang Shen<sup>1</sup>, Hui-Chi Huang<sup>5</sup>, Tsung-Lin Li<sup>3</sup>,  
Kung-Ta Lee<sup>2\*</sup>, Yao-Haur Kuo<sup>1,6\*</sup> and Chia-Ching Liaw<sup>1,7\*</sup>

<sup>1</sup>National Research Institute of Chinese Medicine, Taipei, Taiwan, <sup>2</sup>Department of Biochemical Science and Technology, National Taiwan University, Taipei, Taiwan, <sup>3</sup>Genomics Research Center, Academia Sinica, Taipei, Taiwan, <sup>4</sup>Institute of Physiology, School of Medicine, National Yang Ming Chiao Tung University, Taipei, Taiwan, <sup>5</sup>Department of Chinese Pharmaceutical Sciences and Chinese Medicine Resources, China Medical University, Taichung, Taiwan, <sup>6</sup>Graduate Institute of Integrated Medicine, College of Chinese Medicine, China Medical University, Taichung, Taiwan, <sup>7</sup>Department of Biochemical Science and Technology, National Chiayi University, Chiayi, Taiwan

*Mesona procumbens* Hemsley is a plant conventionally processed to provide popular food materials and herbal medicines in Asia. In this study, six triterpene acids, including five new ones (mesonaic acids D-H, **1–5**), and one proximadiol-type sesquiterpene (**7**) were isolated from the methanolic extract of the air-dried *M. procumbens*. Chemical structures of **1–7** were established by spectroscopic methods, especially 2D NMR techniques (<sup>1</sup>H–<sup>1</sup>H COSY, HSQC, HMBC, and NOESY) and HRESIMS. Concerning their biological activities, compounds **1**, **2**, **6**, and **7** were examined manifesting high inhibition toward the pro-inflammatory NO production with EC<sub>50</sub> values ranging from 12.88 to 21.21 μM, outrunning the positive control quercetin (24.12 μM). The mesoeudesmol B (**7**) identified from *M. procumbens* is the very first example, which exhibited high anti-inflammatory activity diminishing the level of the lipopolysaccharide-induced NO in RAW264.7 macrophage cells, thereby suppressing the secretion of pro-inflammatory cytokines TNF-α and IL-6 and the level of two critical downstream inflammatory mediators iNOS and COX-2.

## KEYWORDS

*Mesona procumbens* Hemsley, triterpene acid, mesonaic acid, sesquiterpene, mesoeudesmol, anti-inflammatory

## 1 Introduction

*Mesona procumbens* Hemsley (Hsian-tsao), an annual herb belonging to the Lamiaceae family, is distributed in the tropical and subtropical regions of South Asia, such as Taiwan, Indonesia, Thailand, Vietnam, and southern China (Feng et al., 2012). This herb is conventionally used alone as a heat-clearing (Qingre) and detoxifying (Jiedu) agent or filled in a prescription of traditional Chinese medicine typically for the treatment of heat-shock, hypertension, diabetes, hepatic disease, and various inflammations, such as joint and muscle pains (Yen and Hung, 2000; Hung and Yen, 2002). Hsian-tsao (also

known as grass jelly herb) is preferably consumed as herbal tea, herbal jelly dessert (grass jelly), or dessert soup given its unique smell, refreshing taste, and medicinal benefits from the major component, polysaccharide gum, which is the most attractive target in this edible plant (Lai and Liao, 2002; Lai et al., 2003; Zhuang et al., 2010). Recent studies further revealed that the Hsian-tso aqueous extract can stop disease progression of liver fibrosis through its apoptotic effects on the activation of hepatic stellate cells (Yeh et al., 2019). The crude polysaccharides from Hsian-tso demonstrated a wound healing activity in the streptozotocin-induced diabetic mouse model (Fan et al., 2021). Numerous pharmacological properties, such as anti-inflammatory (Huang et al., 2012), antioxidant (Lin et al., 2018), antihypertensive (Yeh et al., 2009), antimutagenic (Yen et al., 2001), DNA damage protection (Yen et al., 2000), liver fibrosis prevention (Shyu et al., 2008), and renal protective activities, from *M. procumbens* extracts have been independently reported from time to time (Yang et al., 2008). In addition, some such chronic inflammations such as cardiovascular, cancer, diabetes, arthritis, pulmonary, and autoimmune diseases reported (Singh et al., 2019) can be improved by natural products for they possess some yet-unknown chemo-preventive activities (Azab et al., 2016; Huang et al., 2021).

This study aimed at investigating untapped anti-inflammatory ingredients from Hsian-tso rather than the known polysaccharide gum. Seven new chemical entities were identified herein, including five new triterpene acids (two 24-nor-oleanane-type triterpenes 1–2, one 24-nor-ursane-type triterpene 3, one ursane-type triterpene acid 4, and one ursane-type *seco*-triterpene acid 5), one known 2 $\alpha$ ,3 $\alpha$ ,19 $\alpha$ -trihydroxy-24-norursic acid (23), 12-dien-28-oic acid (6), and one new proximadiol (cryptomeridiol)-type sesquiterpene 7 isolated from the methanolic extract of *M. procumbens*. Having identified their chemical structures, these compounds were subjected to biochemical assay for evaluating their anti-inflammatory capacities against the lipopolysaccharide-induced NO production in RAW264.7 macrophage cells.

## 2 Materials and methods

### 2.1 General experimental procedures

Optical rotations were determined by a JASCO P-2000 polarimeter at 25°C. Infrared (IR) spectra were recorded on a Thermo Scientific Nicolet iS5 FTIR spectrometer. The ECD spectra were measured by a JASCO J-715 spectropolarimeter. High-resolution electrospray ionization mass spectrometry (HRESIMS) data were established by a Thermo Scientific Ultimate 3000 UHPLC System with a Thermo Scientific Q Exactive™ Focus Hybrid Quadrupole-Orbitrap Mass Spectrometer. NMR (nuclear magnetic resonance) spectra,

including  $^1\text{H}$ ,  $^{13}\text{C}$ , DEPT,  $^1\text{H}$ - $^1\text{H}$  COSY, HMBC, HSQC, and NOESY, were recorded on Varian Unity Inova 500 MHz (5 mm SWPFG/TRPFG probe) or Varian VNMRs 600 MHz spectrometers (cold probe) and the chemical shifts were referenced by deuterated solvent methanol- $d_4$ . Silica gel 60 (Merck, 70–230 and 230–400 meshes),  $\text{C}_{18}$  gel (Chromatorex, 40–75 mesh), Diaion HP-20 (Mitsubishi Chemical Co.), and Sephadex LH-20 (GE) were used for column chromatography. Preparative HPLC (high-performance liquid chromatography) was performed using a Shimadzu LC-8A pump and an SPD-10A VP UV detector (210 and 254 nm wavelengths) with a Cosmosil 5 $\text{C}_{18}$  AR-II column (250 × 20 mm, Nacalai Tesque). TLC (thin-layer chromatography) analyses were conducted on pre-coated silica gel plates (Merck, Kieselgel 60 F $_{254}$ , 1 mm) and sprayed with anisaldehyde-sulfuric acid reagent and then heated at 100°C.

### 2.2 Plant material

The whole plants of the air-dried *M. procumbens* Hemsley (8.0 kg) were purchased from Starsci Biotech company in September 2019. A voucher specimen (No. NRICM-20190901) was deposited in the Herbarium of Division of Chinese Materia Medica Development, NRICM, Taipei, Taiwan.

### 2.3 Extraction, isolation, and purification

The air-dried plant of *M. procumbens* Hemsley (8.0 kg) was shredded into 5 mm and extracted with methanol (80 L) at 50°C thrice, and the combined extract was concentrated under reduced pressure removing methanol to obtain the methanolic crude extract. The crude extract (ca. 796.5 g) was dissolved in ddH $_2$ O and then the aqueous solution was further sequentially partitioned with *n*-hexane and dichloromethane ( $\text{CH}_2\text{Cl}_2$ ) to obtain the hexane,  $\text{CH}_2\text{Cl}_2$ , and aqueous extracts. The  $\text{CH}_2\text{Cl}_2$  extract (ca. 47.6 g) was fractionated by a  $\text{C}_{18}$  gel flash column (15 × 25 cm) eluting with a 20%, 40%, 60%, 80%, 90%, and 100% MeOH/H $_2$ O, successively, to yield six fractions (Fr. I–VI). Fr. IV was separated by chromatography on a flash column (silica gel, 60–230 mesh, 15 × 20 cm) eluting with  $\text{CH}_2\text{Cl}_2$  and acetone (from 5% to 100% acetone) to obtain eight subfractions (Fr. IVA ~ H). Fr. IVF was separated by preparative HPLC on a Cosmosil 5 $\text{C}_{18}$  AR-II column (250 × 20 mm, flow rate: 10.0 ml/min) with 60% acetonitrile (ACN) in H $_2$ O to afford seven subfractions (Fr. IVF-1~7). Fr. IVF-4 was further purified by HPLC with Cosmosil 5 $\text{C}_{18}$  AR-II column (flow rate: 10.0 ml/min), eluting with 45% ACN to afford 2 (2.1 mg,  $R_f$ : 33.7 min). Using the same HPLC and RP column, eluting with 50% ACN, compound 5 (2.6 mg,  $R_f$ : 21.3 min) was purified. Fr. IVE was fractionated by HPLC (Cosmosil 5 $\text{C}_{18}$  AR-II column, 250 × 20 mm, flow rate: 10.0 ml/min) with 55% ACN to afford eight subfractions (Fr.

TABLE 1 <sup>1</sup>H-NMR spectroscopic data of 1–6 in methanol-*d*<sub>4</sub>.

No	1 <sup>a</sup>	2 <sup>a</sup>	3 <sup>a</sup>	4 <sup>a</sup>	5 <sup>b</sup>	6 <sup>a</sup>
1	1.35 m	1.23 dd (12.0, 12.6)	2.14 brd (16.2)	1.34 m	2.39 d (18.0)	1.38 m
	1.70 dd (4.8, 12.0)	1.67 dd (6.6, 12.6)	2.55 d (16.2)	1.53 m	2.58 d (18.0)	1.71 m
2	3.65 ddd (3.6, 4.8, 12.0)	3.68 ddd (3.6, 4.8, 11.4)	-	3.89 ddd (3.0, 4.8, 12.0)	-	3.67 ddd (3.6, 4.8, 12.0)
3	4.12 d (3.6)	4.11 d (3.6)	-	3.73 brd (3.0)	-	4.13 d (3.6)
5	2.17 dd (4.2, 9.6)	2.22 br d (13.2)	2.41 brd (12.0)	1.91 m	2.53 dd (3.0, 12.5)	2.18 m
6	1.46 m (2H)	1.48 m	1.47 m	1.43 m (2H)	1.53 m	1.46 m (2H)
		1.62 m	1.88 m		1.35 m	
7	1.34 m	1.32 m	1.43 m	1.23 m	1.35 m	1.34 m
	1.58 m	1.98 td (3.0, 13.2)	1.71 td (4.2, 12.6)	1.74 m	1.66 m	1.63 m
9	1.82 m	1.21 m	2.05 m	1.94 m	2.76 dd (6.5, 11.5)	1.93 m
11	1.94 m	1.32 m	2.03 m (2H)	1.96 m	1.99 m	1.98 m
	2.02 m	1.55 m	-	2.02 m	2.08 m	2.14 m
12	5.28 t (3.6)	4.00 brdd (2.4, 5.4)	5.33 t (3.6)	5.28 t (3.6)	5.31 t (4.0)	5.30 t (3.0)
15	1.10 m	5.02 d (5.4)	1.06 m	0.99 m	1.10 m	1.01 brd (13.8)
	1.80 m		1.81 m	1.79 td (5.4, 13.8)	1.89 m	1.83 td (4.8, 13.8)
16	1.61 m	1.64 m	1.83 m	1.50 m	1.90 m	1.52 m
	2.02 m	2.13 d (12.6)	2.56 td (4.2, 12.6)	2.57 td (4.8, 13.2)	2.28 m	2.58 td (4.8, 13.2)
18	2.88 dd (4.8, 14.4)	1.88 dd (4.2, 12.6)	2.69 brs	2.49 brs	2.49 brs	2.50 brs
19	1.08 m	1.18 m	-	-	-	-
	1.80 m	1.82 dd (4.8, 13.8)	-	-	-	-
20	-	-	1.57 m	1.33 m	1.50 m	1.34 m
21	1.15 m	1.09 td (4.2, 13.2)	3.90 dd (3.0, 6.0)	1.22 m	1.45 dd (4.5, 12.5)	1.22 m
	1.48 m	1.30 m	-	1.71 m	1.85 dd (12.0, 12.5)	1.71 m
22	1.57 m	1.17 m	1.81 m	1.60 td (4.8, 13.8)	3.71 dd (4.5, 12.0)	1.61 m
	1.67 m	2.09 td (4.2, 15.0)	2.10 dd (3.0, 14.4)	1.71 m	-	1.72 m
23	4.67 brs	4.99 brs	1.84 d (1.8)	1.19 s	1.29 s	4.68 brs
	5.00 brs	4.85 brs	-	-	-	5.01 brs
24	-	-	-	-	1.28 s	-
25	0.76 s	0.66 s	0.93 s	1.03 s	1.08 s	0.78 s
26	0.86 s	1.17 s	0.88 s	0.79 s	0.85 s	0.84 s
27	1.21 s	0.74 d (7.2)	1.36 s	1.38 s	1.40 s	1.36 s
28	-	1.19 m	-	-	-	-
29	0.92 s	0.94 s	1.16 s	1.18 s	1.17 s	1.19 s
30	3.18 brs (2H)	0.98 s	1.16 d (6.6)	0.92 d (6.6)	0.98 d (6.5)	0.92 d (6.6)

<sup>a</sup><sup>1</sup>H-NMR data were recorded on 600 MHz.<sup>b</sup><sup>1</sup>H-NMR data were recorded on 500 MHz.

IVE-1~8). Fr. IVE-3 was further purified again with 45% ACN (flow rate: 10.0 ml/min) to yield **3** (1.9 mg, *R*<sub>t</sub>: 18.3 min). Fr. IVD was subjected to preparative HPLC with 45% ACN (flow rate: 10.0 ml/min) to yield six subfractions (Fr. IVD-1~6). Fr. IVD-4 was further repeatedly purified with 40% ACN (flow rate: 10.0 ml/min) to afford compounds **4** (2.3 mg, *R*<sub>t</sub>: 17.9 min) and **7** (4.8 mg, *R*<sub>t</sub>: 26.2 min). Fr. IVC was subjected to HPLC with 45% ACN (flow rate: 10.0 ml/min) to divide into eight subfractions (Fr. IVC-1~5). Fr. IVC-2 was separated by a Cosmosil 5C<sub>18</sub> AR-II column (flow rate: 10.0 ml/min) to afford **1** (1.6 mg, *R*<sub>t</sub>: 31.2 min). Fr. IVC-4 was also purified by

HPLC using the same RP column with 40% ACN (flow rate: 10.0 ml/min) to afford **6** (2.5 mg, *R*<sub>t</sub>: 49.9 min).

## 2.4 Spectroscopic data

### 2.4.1 Mesonaic acid D (**1**)

White amorphous powder; [ $\alpha$ ] +12.9 (*c* 0.5, MeOH); IR (KBr)  $\nu_{\max}$  3402, 2927, 1694, 1437, 1316, 1017 cm<sup>-1</sup>; <sup>1</sup>H- (600 MHz) and <sup>13</sup>C- (150 MHz) NMR spectroscopic data (methanol-*d*<sub>4</sub>) are shown in Tables 1, 2, respectively;

TABLE 2 <sup>13</sup>C-NMR spectroscopic data of 1–6 in methanol-*d*<sub>4</sub>.

No	1 <sup>a</sup>	2 <sup>a</sup>	3 <sup>a</sup>	4 <sup>a</sup>	5 <sup>b</sup>	6 <sup>a</sup>
1	42.0	CH <sub>2</sub>	42.1	CH <sub>2</sub>	51.8	CH <sub>2</sub>
2	68.7	CH	68.8	CH	194.2	qC
3	75.6	CH	75.4	CH	143.9	qC
4	151.0	qC	150.5	qC	131.6	qC
5	44.4	CH	45.1	CH	48.5	CH
6	20.0	CH <sub>2</sub>	19.9	CH <sub>2</sub>	20.5	CH <sub>2</sub>
7	31.1	CH <sub>2</sub>	37.0	CH <sub>2</sub>	32.0	CH <sub>2</sub>
8	39.3	qC	39.5	qC	39.1	qC
9	45.0	CH	43.2	CH	43.4	CH
10	37.3	qC	36.9	qC	40.9	qC
11	23.9	CH <sub>2</sub>	28.9	CH <sub>2</sub>	23.4	CH <sub>2</sub>
12	122.4	CH	73.0	CH	128.0	CH
13	144.1	qC	33.8	qC	138.2	qC
14	41.8	qC	36.1	qC	41.6	qC
15	27.3	CH <sub>2</sub>	78.0	CH	28.4	CH <sub>2</sub>
16	22.6	CH <sub>2</sub>	33.0	CH <sub>2</sub>	27.6	CH <sub>2</sub>
17	46.5	qC	45.2	qC	47.2	qC
18	40.7	CH	39.2	CH	54.1	CH
19	39.9	CH <sub>2</sub>	41.0	CH <sub>2</sub>	75.2	qC
20	35.4	qC	29.5	qC	41.8	CH
21	27.9	CH <sub>2</sub>	34.2	CH <sub>2</sub>	73.1	CH
22	31.7	CH <sub>2</sub>	27.7	CH <sub>2</sub>	43.4	CH <sub>2</sub>
23	109.4	CH <sub>2</sub>	109.0	CH <sub>2</sub>	11.9	CH <sub>3</sub>
24						178.5
25	13.0	CH <sub>3</sub>	13.5	CH <sub>3</sub>	13.0	CH <sub>3</sub>
26	16.4	CH <sub>3</sub>	20.0	CH <sub>3</sub>	16.3	CH <sub>3</sub>
27	25.1	CH <sub>3</sub>	15.7	CH <sub>2</sub>	22.5	CH <sub>3</sub>
28	180.3	qC	182.3	qC	180.1	qC
29	18.1	CH <sub>3</sub>	32.0	CH <sub>3</sub>	25.1	CH <sub>3</sub>
30	73.0	CH <sub>2</sub>	22.7	CH <sub>3</sub>	12.5	CH <sub>3</sub>

<sup>a</sup><sup>13</sup>C- and DEPT NMR data were recorded on 150 MHz.<sup>b</sup><sup>13</sup>C- and DEPT NMR data were recorded on 125 MHz.

HRESIMS *m/z* 495.3097 [M + Na]<sup>+</sup> (calcd. for C<sub>29</sub>H<sub>44</sub>O<sub>5</sub>Na, 495.3081).

#### 2.4.2 Mesonaic acid E (2)

White amorphous powder; [α] +19.7 (*c* 0.5, MeOH); IR (KBr)  $\nu_{\max}$  3399, 2930, 1744, 1390, 1245, 1012 cm<sup>-1</sup>; <sup>1</sup>H- (600 MHz) and <sup>13</sup>C- (150 MHz) NMR spectroscopic data (methanol-*d*<sub>4</sub>) are shown in Tables 1, 2, respectively; HRESIMS *m/z* 469.2965 [M – H]<sup>–</sup> (calcd. for C<sub>29</sub>H<sub>41</sub>O<sub>5</sub>, 469.2949).

#### 2.4.3 Mesonaic acid F (3)

White amorphous powder; [α] +25.1 (*c* 0.5, MeOH); IR (KBr)  $\nu_{\max}$  3369, 2936, 1712, 1630, 1385, 1170, 1017 cm<sup>-1</sup>; <sup>1</sup>H- (600 MHz) and <sup>13</sup>C- (150 MHz) NMR spectroscopic data (methanol-*d*<sub>4</sub>) are shown in Tables 1, 2, respectively;

HRESIMS *m/z* 485.2919 [M – H]<sup>–</sup> (calcd. for C<sub>29</sub>H<sub>41</sub>O<sub>6</sub>, 485.2898).

#### 2.4.4 Mesonaic acid G (4)

White amorphous powder; [α] +23.4 (*c* 0.5, MeOH); IR (KBr)  $\nu_{\max}$  3402, 2927, 1687, 1235, 1022 cm<sup>-1</sup>; <sup>1</sup>H- (600 MHz) and <sup>13</sup>C- (150 MHz) NMR spectroscopic data (methanol-*d*<sub>4</sub>) are shown in Tables 1, 2, respectively; HRESIMS *m/z* 517.3176 [M – H]<sup>–</sup> (calcd. for C<sub>30</sub>H<sub>45</sub>O<sub>7</sub>, 517.3160).

#### 2.4.5 Mesonaic acid H (5)

White amorphous powder; [α] +27.3 (*c* 0.5, MeOH); IR (KBr)  $\nu_{\max}$  3414, 2952, 1707, 1462, 1163, 1027 cm<sup>-1</sup>; <sup>1</sup>H- (500 MHz) and <sup>13</sup>C- (125 MHz) NMR spectroscopic data (methanol-*d*<sub>4</sub>) are shown in Tables 1, 2, respectively; HRESIMS *m/z* 533.3124 [M – H]<sup>–</sup> (calcd. for C<sub>30</sub>H<sub>45</sub>O<sub>8</sub>, 533.3109).

TABLE 3  $^1\text{H}$ - and  $^{13}\text{C}$ -NMR spectroscopic data of **7** in methanol- $d_4$ .

No	$^1\text{H}$ NMR (600 MHz)	$^{13}\text{C}$ NMR (150 MHz)		No	$^1\text{H}$ NMR (600 MHz)	$^{13}\text{C}$ NMR (150 MHz)	
1	1.31 m 1.88 m	46.0	$\text{CH}_2$	12	3.46 s (2H)	67.7	$\text{CH}_2$
2	5.18 ddd (4.2, 7.8, 12.0)	69.3	CH	13	1.12 s	19.7	$\text{CH}_3$
3	1.62 m 2.21 ddd (2.4, 4.2, 12.0)	47.7	$\text{CH}_2$	14	1.19 brs	22.0	$\text{CH}_3$
4	-	72.0	qC	15	1.02 s	18.5	$\text{CH}_3$
5	1.34 m	53.8	CH	1'	-	166.0	qC
6	1.45 m 1.65 m	20.7	$\text{CH}_2$	2'	-	130.4	qC
7	1.58 m	44.5	CH	3'	7.98 dd (1.8, 8.0)	129.0	CH
8	1.12 m 1.88 m	21.1	$\text{CH}_2$	4'	7.45 dd (7.2, 8.0)	128.1	CH
9	1.27 m 1.54 m	44.3	$\text{CH}_2$	5'	7.58 m	132.7	CH
10	-	33.9	qC	6'	7.45 dd (7.2, 8.0)	128.1	CH
11	-	74.0	qC	7'	7.98 dd (1.8, 8.0)	129.0	CH

#### 2.4.6 $2\alpha,3\alpha,19\alpha$ -Trihydroxy-24-norursa-4(23),12-dien-28-oic acid (**6**)

White amorphous powder;  $[\alpha] +21.8$  (*c* 0.5, MeOH); IR (KBr)  $\nu_{\text{max}}$  3470, 2947, 1697, 1459, 1247, 1039  $\text{cm}^{-1}$ ;  $^1\text{H}$ - (600 MHz) and  $^{13}\text{C}$ - (150 MHz) NMR spectroscopic data (methanol- $d_4$ ) are shown in Tables 1, 2, respectively; HRESIMS  $m/z$  495.3072  $[\text{M} + \text{Na}]^+$  (calcd. for  $\text{C}_{29}\text{H}_{44}\text{O}_5\text{Na}$ , 495.3081).

#### 2.4.7 Mesoeudesmol B (**7**)

Colorless oil;  $[\alpha] +9.1$  (*c* 0.5, MeOH); IR (KBr)  $\nu_{\text{max}}$  3389, 2932, 1716, 1455, 1388, 1279, 1116, 1025  $\text{cm}^{-1}$ ; UV  $\lambda_{\text{max}}$  (MeOH) (log  $\epsilon$ ) 273 (2.98), 229 (3.82) nm;  $^1\text{H}$ - (600 MHz) and  $^{13}\text{C}$ - (150 MHz) NMR spectroscopic data (methanol- $d_4$ ) are shown in Table 3; HRESIMS  $m/z$  399.2148  $[\text{M} + \text{Na}]^+$  (calcd. for  $\text{C}_{22}\text{H}_{32}\text{O}_5\text{Na}$ , 399.2142).

### 2.5 Dimolybdenum tetraacetate $[\text{Mo}_2(\text{OAc})_4]$ -modified circular dichroism analysis

The determination of the absolute configuration of cyclic and acyclic *vic*-diols was achieved by employing a transition metal chelate reagent, dimolybdenum tetraacetate  $[\text{Mo}_2(\text{OAc})_4]$ . Compound **7** was directly dissolved in a solution of  $\text{Mo}_2(\text{OAc})_4$  complex in DMSO in a molar ratio of  $\text{Mo}_2(\text{OAc})_4/\text{compound}$  of about 1:0.3–1:0.7, and the mixture was subsequently measured for the induced CD spectra without the preparation and isolation of the complexes.

### 2.6 Cell culture and viability assay

The RAW264.7 mouse macrophages were purchased from the Food Industry Research and Development Institute (Hsinchu, Taiwan). Cells were cultured in DMEM supplemented with 10% heat-inactivated FBS in a 5%  $\text{CO}_2$  humidified incubator at 37°C. For viability assay, RAW264.7 cells were pretreated with various concentrations of the isolated compounds (0, 5, 10, and 20  $\mu\text{M}$ ) 1 h prior to LPS (1  $\mu\text{g}/\text{ml}$ ) stimulation. After 24 h treatment, cell viability was determined by Cell Counting Kit-8 (Dojindo, Rockville, MD, United States) according to the manufacturer's instructions.

### 2.7 NO releasing inhibition assay

Griess reagent (1% sulfanilamide in 5% phosphoric acid and 0.1% naphthylethylenediamine dihydrochloride in water) was used to determine NO production. RAW264.7 cells were pretreated in the same manner described in cell viability assay. 100  $\mu\text{L}$  of supernatant of each pretreated cell solution was transferred to a new microtiter plate, and each supernatant was mixed with 100  $\mu\text{L}$  of Griess reagent. The microtiter plate was left at room temperature for 10 min for color development, and each solution was measured by a microplate reader at UV 540 nm. All experiments were performed in triplicate.

## 2.8 Western blot analysis

RAW264.7 cells were pretreated with compound **7** (0, 5, 10, or 20  $\mu\text{M}$ ) or quercetin (25  $\mu\text{M}$ , Sigma-Aldrich) for 1 h and then stimulated with LPS for an additional 24 h. The cells were lysed in radioimmunoprecipitation assay (RIPA) lysis buffer and protein concentration was determined using the Bradford assay (Bio-Rad Laboratories, Munich, Germany). The protein lysates were separated by SDS-PAGE and then transferred to a PVDF membrane. The blot was blocked with TBS containing 5% nonfat milk for 1 h at room temperature and then incubated with primary antibodies to iNOS, COX-2 or  $\beta$ -actin at 4°C overnight. The blots were washed three times with 0.1% TBST (0.1% Tween 20 in TBS) and then incubated with a peroxidase-conjugated secondary antibody for 1 h at room temperature. After washing, the protein bands were detected using an ECL reagent and X-ray film.

## 2.9 Determination of IL-6 and TNF- $\alpha$ levels

The measurement of the IL-6 and TNF- $\alpha$  levels was performed using commercial ELISA kits (RAB0308-1KT and RAB0477-1KT (Sigma Chemical Co., St. Louis, MO, United States), respectively) according to the manufacturer's instructions. Briefly, samples and standards were added to antibody-coated 96 wells and were incubated for 2.5 h at room temperature. After incubation, wells were washed with wash buffer four times, and then detection antibody was added and incubated for another 1 h at room temperature. After washing, 3,3',5,5'-tetramethylbenzidine (TMB) substrate was added and incubated in the dark for 30 min at room temperature followed by adding stop solution and reading absorbance at 450 nm immediately.

## 2.10 Statistical analysis

Statistical analyses were performed using SPSS (SPSS, Chicago, IL, United States). Data are expressed as the mean  $\pm$  standard deviations. Statistical significance was determined using one-way ANOVA analysis followed by Tukey's test. *p*-values < 0.05 were considered statistically significant.

## 3 Results and discussion

The methanolic extract of *M. procumbens* was dried and resuspended in  $\text{H}_2\text{O}$ ; this aqueous solution was extracted by *n*-hexane and  $\text{CH}_2\text{Cl}_2$  to give rise to two organic layers. The  $\text{CH}_2\text{Cl}_2$  portion was subjected to chromatography by a flash column and preparative RP-HPLC to afford five new and one known triterpene acids (**1–6**), together with one brand new

sesquiterpene (**7**) (Figure 1). All pure components (**1–7**) were then evaluated for their anti-inflammatory activities using an *in vitro* LPS-stimulated murine macrophage model.

## 3.1 Structural elucidation of the isolated compounds

Compound **1** ( $[\alpha]_D^{25} +12.9$ ,  $c = 0.5$ , MeOH), a colorless amorphous powder, has a molecular formula of  $\text{C}_{29}\text{H}_{44}\text{O}_5$  with 8 degrees of unsaturation (DOU) deduced from the sodiated HRESIMS pseudo-ion at  $m/z$  495.3097  $[\text{M} + \text{Na}]^+$  (calcd. for  $\text{C}_{29}\text{H}_{44}\text{O}_5\text{Na}$ , 495.3081). In  $^1\text{H-NMR}$  spectrum (Table 1), four tertiary methyl signals ( $\delta_{\text{H}}$  0.76, 0.86, 0.92, and 1.21 s), one olefinic methylene signal ( $\delta_{\text{H}}$  4.67 brs and 5.00 brs), and one olefinic methine signal ( $\delta_{\text{H}}$  5.28 t,  $J = 3.6$  Hz) were observed. Based on  $^{13}\text{C-NMR}$  and DEPTs spectra (Table 2), the 29 carbons can be categorized into 4 methyls, 11 methylenes (one oxymethylene at  $\delta_{\text{C}}$  73.0 and one olefinic methylene at  $\delta_{\text{C}}$  109.4), 6 methines (two oxymethines at  $\delta_{\text{C}}$  68.7 and 75.6 as well as one olefinic methine at  $\delta_{\text{C}}$  122.4), and 8 quaternary carbons (two  $\text{sp}^2$  quaternary carbons at  $\delta_{\text{C}}$  144.1 and 151.0 and one carboxylic acid group at  $\delta_{\text{C}}$  180.3). The above two olefins and one carboxyl group accounted for three DOU, and the remaining five constrained **1** to a pentacyclic structure. The assignments of  $^1\text{H-}$  and  $^{13}\text{C-NMR}$  spectroscopic data were completed by a combination of HSQC,  $^1\text{H-}^1\text{H}$  COSY, and HMBC experiments. By comparison of carbon signals of **1** with that of oleanolic acid along with the analysis of the COSY and HMBC correlations of **1** altogether determined the carbon skeleton of **1**, an oleanane-type nortriterpenoid (Kashiwada et al., 1998). In Figure 2, the COSY correlations of H-2 ( $\delta_{\text{H}}$  3.65 ddd,  $J = 3.6, 4.8, 12.0$  Hz)/H-3 ( $\delta_{\text{H}}$  4.12 d,  $J = 3.6$  Hz) confirmed that the attachments of these two hydroxyls are at C-2 and C-3, whereas the HMBC correlations from H<sub>2</sub>-30 ( $\delta_{\text{H}}$  3.18 brs) to C-19 ( $\delta_{\text{C}}$  39.9), C-20 ( $\delta_{\text{C}}$  35.4), and C-21 ( $\delta_{\text{C}}$  27.9) revealed a primary alcohol at C-30. Furthermore, an *exo*-4 (23)-double bond was verified according to the HMBC correlations of olefinic methylene H<sub>2</sub>-23 to C-3 ( $\delta_{\text{C}}$  75.6), C-4 ( $\delta_{\text{C}}$  151.0), and C-5 ( $\delta_{\text{C}}$  44.4); the tri-substituted  $\Delta^{12}$  double bond was confirmed by the COSY correlations of H-9 ( $\delta_{\text{H}}$  1.82 m)/H<sub>2</sub>-11 ( $\delta_{\text{H}}$  1.94 and 2.02 m)/H-12 ( $\delta_{\text{H}}$  5.28 t,  $J = 3.6$  Hz) and by the HMBC correlations from H-18 ( $\delta_{\text{H}}$  2.88 dd,  $J = 4.8$  and 14.4 Hz) to C-12 ( $\delta_{\text{C}}$  122.4), C-13 ( $\delta_{\text{C}}$  144.1), and C-14 ( $\delta_{\text{C}}$  41.8). The spectroscopic evidence altogether indicated that **1** is a new 24-noroleanane-type triterpene acid.

The pentacyclic moiety of oleanane-type triterpenoids is rigid, showing the configurations with those of regular oleanane-type triterpenoids based on NOESY experiment, which provides clear assignments. The NOESY correlations of H-5/H-9, H-9/ $\text{CH}_3$ -27,  $\text{CH}_3$ -27/ $\text{H}_\alpha$ -19, and  $\text{H}_\alpha$ -19/H<sub>2</sub>-30 indicated  $\alpha$ -orientations, whereas those of  $\text{CH}_3$ -25,  $\text{CH}_3$ -26, H-18, and  $\text{CH}_3$ -29 presented  $\beta$ -directions with regard to H-18/ $\text{CH}_3$ -25,  $\text{CH}_3$ -25/ $\text{CH}_3$ -26, and H-18/ $\text{CH}_3$ -29 (Figure 3).

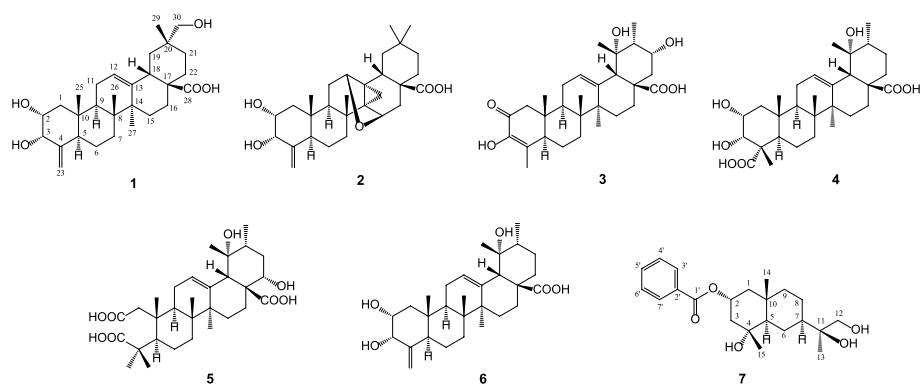


**FIGURE 1**  
Chemical structures of compounds **1–7** isolated from *M. procumbens*.

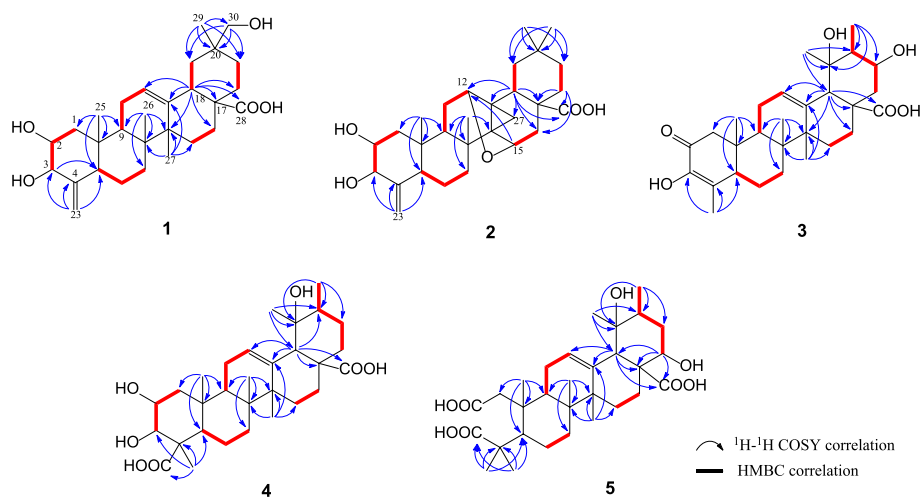


**FIGURE 2**  
 $^1\text{H}$ - $^1\text{H}$  COSY and key HMBC correlations of triterpene acids **1–5**.

Meanwhile, the NOESY correlations of H-2/H-3 and H-2/CH<sub>3</sub>-25 and the small proton constant of H-3 ( $^3J_{\text{H-2,H-3}} = 3.6$  Hz) agreed with the  $\alpha$ -oriented OH-2 and OH-3 within a *cis*-relationship. As a result, the chemical structure of mesonaic acid D (**1**) was established as 2 $\alpha$ ,3 $\alpha$ ,30-trihydroxy-24-norolean-4(23),12-dien-28-oic acid.

Mesonaic acid E (**2**) was white amorphous powders with  $[\alpha] +19.7$  (*c* 0.5, MeOH). The molecular formula C<sub>29</sub>H<sub>42</sub>O<sub>5</sub> on par with 9 DOU was deduced based on a quasimolecular ion at *m/z* 469.2965 [M - H]<sup>-</sup> (calcd. for C<sub>29</sub>H<sub>41</sub>O<sub>5</sub>, 469.2949) in the HRESIMS experiment. The characteristic  $^1\text{H}$ - and  $^{13}\text{C}$ -NMR signals (Tables 1, 2), four tertiary methyls ( $\delta_{\text{H}}$  0.66 s/ $\delta_{\text{C}}$  13.5;  $\delta_{\text{H}}$  0.94 s/ $\delta_{\text{C}}$  32.0;  $\delta_{\text{H}}$  0.98 s/ $\delta_{\text{C}}$  22.7;  $\delta_{\text{H}}$  1.17 s/ $\delta_{\text{C}}$  20.0), two oxymethines C-2 ( $\delta_{\text{H}}$  3.68 ddd,  $J = 3.6, 4.8, 11.4$  Hz/ $\delta_{\text{C}}$  68.8)

and C-3 ( $\delta_{\text{H}}$  4.11 d,  $J = 3.6$  Hz/ $\delta_{\text{C}}$  75.4), one exocyclic methylene involving C-4 ( $\delta_{\text{C}}$  150.5) and C-23 ( $\delta_{\text{H}}$  4.85 brs and 4.99 brs/ $\delta_{\text{C}}$  109.0), and one COOH-28 ( $\delta_{\text{C}}$  180.3) suggested that compound **2** is a derivative of 24-nor-oleanane triterpene acid possessing the same 2,3-diol ring A as **1**. Deduction of DOU from the 4 (23)-double bond, COOH-28, and the pentacyclic ring moiety, there are two DOU unassigned. After a detailed comparison of  $^1\text{H}$ -,  $^{13}\text{C}$ -NMR, and DEPTs spectra, we found that a tri-substituted  $\Delta^{12}$  double bond and the primary alcohol of C-30 disappeared, while two oxymethines ( $\delta_{\text{H}}$  4.00 dd,  $J = 2.4$  and 5.4 Hz/ $\delta_{\text{C}}$  73.0 and  $\delta_{\text{H}}$  5.02 d,  $J = 5.4$  Hz/ $\delta_{\text{C}}$  78.0), one aliphatic methylene ( $\delta_{\text{H}}$  0.74 d,  $J = 7.2$  Hz/ $\delta_{\text{C}}$  15.7), and one aliphatic quaternary carbon ( $\delta_{\text{C}}$  33.8) emerged. By a combination of the COSY correlations of H-9/H<sub>2</sub>-11/H-12 (indicating that olefinic methine C-12 converts to an

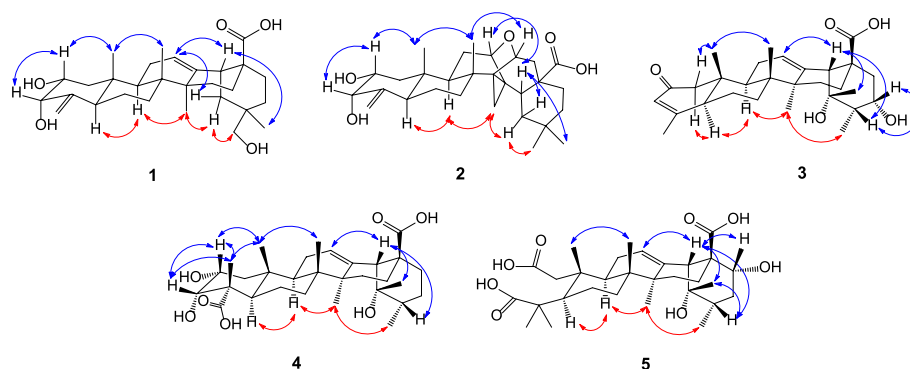


**FIGURE 3**  
Main NOESY correlations of triterpene acids 1–5.

oxymethine) and the HMBC correlations from another oxymethine H-15 to C-12, one DOU was contributed to an oxygen-bridge between C-12 and C-15. The remaining DOU is resulted from a cyclopropane unit assembled by one aliphatic methylene C-27 and two aliphatic quaternary carbons C-13 and C-14, which were confirmed by the HMBC correlations (Figure 2) of H-18 ( $\delta_{\text{H}}$  1.88 dd,  $J = 4.2$  and  $12.6$  Hz)/C-12, C-13, C-17 ( $\delta_{\text{C}}$  45.2), C-27, and COOH-28 and H<sub>3</sub>-26 ( $\delta_{\text{H}}$  1.17 s)/C-7 ( $\delta_{\text{C}}$  37.0), C-8 ( $\delta_{\text{C}}$  39.5), C-9 ( $\delta_{\text{C}}$  43.2), and C-14 ( $\delta_{\text{C}}$  36.1).

In terms of stereochemistry, the chiral centers at ring junctions of **2** are carried on as those at compound **1**; The  $\alpha$ -side of the cyclopropane unit (C-13, C-14, and C-27) which formed via a *si*-attack by  $\alpha$ -oriented CH<sub>3</sub>-27 were supported by the NOESY correlations (H-9/H<sub>2</sub>-27, H<sub>2</sub>-27/H <sub>$\alpha$</sub> -19, and H <sub>$\alpha$</sub> -19/CH<sub>3</sub>-30) (Figure 3). The 2 $\alpha$ ,3 $\alpha$ -diol is also confirmed by the NOESY correlations of H-2/H-3 and H-2/CH<sub>3</sub>-25 as well as the small proton constant of H-3 ( $J = 3.6$  Hz). The configurations of the oxygen bridge heads, C-12 and C-15, were determined to be at the  $\beta$ -side based on the NOESY correlations of H-12/H-18 and H-15/CH<sub>3</sub>-26. Thereby, compound **2** was clearly elucidated as 2 $\alpha$ ,3 $\alpha$ -dihydroxy-12 (15)-epoxy-13 $\alpha$ ,27-cycloolean-4 (23)-en-28-oic acid.

Mesonaic acid **F** (**3**) was obtained as a white powder with specific rotation  $[\alpha] +25.1$  ( $c$  0.5, MeOH). Its IR spectrum showed the presence of a hydroxyl group ( $3369\text{ cm}^{-1}$ ), a carboxyl group ( $1712\text{ cm}^{-1}$ ), a conjugated carbonyl group ( $1630\text{ cm}^{-1}$ ), and an olefinic group ( $1385\text{ cm}^{-1}$ ). The molecular formula of **3** was determined to be C<sub>29</sub>H<sub>42</sub>O<sub>6</sub> (9 DOU) by the given HRESIMS ion at  $m/z$  485.2919 [M – H]<sup>–</sup> (calcd. 485.2898 for C<sub>29</sub>H<sub>41</sub>O<sub>6</sub>). The 29 carbons (Table 2) can be separated into 6 methyls ( $\delta_{\text{C}}$  11.9, 12.5, 13.0, 16.3, 22.5, and 25.1), 7 methylenes ( $\delta_{\text{C}}$  20.5, 23.4, 27.6, 28.4, 32.0, 43.4, and 51.8), 6 methines ( $\delta_{\text{C}}$  41.8, 43.4, 48.5, 54.1, 73.1, and 128.0), and 10 quaternary carbons ( $\delta_{\text{C}}$  39.1, 40.9, 41.6, 47.2, 75.2, 131.6, 138.2, 143.9, 180.1, and 194.2) by <sup>13</sup>C-NMR and DEPTs spectra of **3**. The protons of five methyls [ $\delta_{\text{H}}$  0.88, 0.93, 1.36 s, 1.16 d, ( $J = 6.6$  Hz), and 1.84 d

( $J = 1.8$  Hz)], one oxymethine ( $\delta_{\text{H}}$  3.90 dd,  $J = 3.0$  and  $6.0$  Hz), and one olefinic methine ( $\delta_{\text{H}}$  5.33 t,  $J = 3.6$  Hz) can be clearly observed in <sup>1</sup>H-NMR spectrum (Table 1). Combining the <sup>1</sup>H-, <sup>13</sup>C-NMR, and HSQC experiments, compound **3** was figured out to be a pentacyclic triterpene acid containing one conjugated carbonyl group, one tri-substituted double bond, and one carboxylic acid, reconciling these functional groups and pentacyclic fused ring system with the 9 DOU. The COSY correlations of H-9/H<sub>2</sub>-11/H-12 and the HMBC correlations from a junction proton H-18 ( $\delta_{\text{H}}$  2.69 brs) to C-12, C-13, C-14, C-17 and C-28 together made a tri-substituted double bond at the  $\Delta^{12}$  position clear; the <sup>1</sup>H–<sup>1</sup>H COSY correlations of CH<sub>3</sub>-30/H-20/H-21/H<sub>2</sub>-22 alongside the HMBC correlations of CH<sub>3</sub>-29/C-18, C-19, C-20 illustrated that **3** is a derivative of ursane-type triterpenoids. The most difficult part is that the  $\alpha$ , $\beta$ -unsaturated conjugated carbonyl part in ring A is deduced by the HMBC correlations of CH<sub>3</sub>-23 to C-3, C-4, C-5 and CH<sub>3</sub>-25 to C-1, C-9, C-10, revealing the ursane triterpenoid without the C-24 carbon in **3** (Figure 2). The chiral configurations of **3** were built up by the NOESY correlations (Figure 3) and comparison with a pomolic acid (Kashiwada et al., 1998). As a result, **3** is identified as 3,19 $\alpha$ ,21 $\alpha$ -trihydroxy-2-oxo-24-norurs-3,12-dien-28-oic acid.

Compound **4**,  $[\alpha] +23.4$  ( $c$  0.5, MeOH), was purified as white amorphous powders. The molecular formula C<sub>30</sub>H<sub>46</sub>O<sub>7</sub> (8 DOU) was determined by the HRESIMS molecular ion at  $m/z$  517.3176 [M–H]<sup>–</sup> (calcd. for C<sub>30</sub>H<sub>45</sub>O<sub>7</sub>, 517.3160). The <sup>1</sup>H-, <sup>13</sup>C-NMR (Tables 1, 2), and HSQC spectra of **4** as a whole revealed the presence of six methyls ( $\delta_{\text{H}}$  0.79 s/ $\delta_{\text{C}}$  13.6;  $\delta_{\text{H}}$  0.92 d,  $J = 6.6$  Hz/ $\delta_{\text{C}}$  15.2;  $\delta_{\text{H}}$  1.03 s/ $\delta_{\text{C}}$  15.9;  $\delta_{\text{H}}$  1.18 s/ $\delta_{\text{C}}$  25.6;  $\delta_{\text{H}}$  1.19 s/ $\delta_{\text{C}}$  16.2; and  $\delta_{\text{H}}$  1.38 s/ $\delta_{\text{C}}$  23.6), one tri-substituted olefinic double bond ( $\delta_{\text{H}}$  5.28 t,  $J = 3.6$  Hz/ $\delta_{\text{C}}$  127.8 and  $\delta_{\text{C}}$  138.8), and two carboxyl groups ( $\delta_{\text{C}}$  178.5 and 180.8), the characteristics of urs-12-ene or olean-12-ene derivatives. In addition, two secondary hydroxyl groups at the C-2 and C-3 positions were amended for **4** because of the (C)–CH<sub>2</sub>–CHOH–CHOH–(C) structural moiety

( $\delta_{\text{H}}$  1.34 and 1.53 m; 3.89 ddd,  $J = 3.0, 4.8,$  and  $12.0$  Hz;  $\delta_{\text{H}}$  3.73 brd,  $J = 3.0$  Hz) established by COSY spectrum. The HMBC spectrum of **4** confirmed the above deductions. Furthermore, the two carboxyl groups were assigned at C-24 ( $\delta_{\text{C}}$  180.8) and C-28 ( $\delta_{\text{C}}$  178.5) according to the HMBC correlations from H-18 ( $\delta_{\text{H}}$  2.49 brs) to C-17 ( $\delta_{\text{C}}$  47.6) and carboxyl carbon C-28 ( $\delta_{\text{C}}$  180.8), from CH<sub>3</sub>-23 to two oxymethine carbons [C-3 ( $\delta_{\text{C}}$  75.4) and C-4 ( $\delta_{\text{C}}$  51.8)], carboxyl carbon C-24 ( $\delta_{\text{C}}$  178.5), respectively. The HMBC correlation from CH<sub>3</sub>-29 to oxygen-bearing quaternary carbon C-19 ( $\delta_{\text{C}}$  72.1) put forward that the tertiary hydroxyl group is at C-19 (Figure 2). The configuration of **4** was established by the NOESY correlations (Figure 3) and the coupling constant interpretations for the relevant protons. The 2 $\alpha$ ,3 $\alpha$ -configurations of the two secondary hydroxyl groups of **4** were ascertained by the NOESY correlations of H-2/H-3, H-2/CH<sub>3</sub>-25, H-3/CH<sub>3</sub>-23, CH<sub>3</sub>-23/CH<sub>3</sub>-25, and the small proton coupling constant of H-3 ( $J = 3.6$  Hz) agreed with their directions. These elucidations led compound **4** to 2 $\alpha$ ,3 $\alpha$ ,19 $\alpha$ -trihydroxyurs-12-ene-24,28-dioic acid, a triterpene acid monomer named mesonaic acid G, the first of its kind isolated from *M. procumbens* (it was reported to be a unit in the dimeric triterpene glucoside sanguidioside A) (Liu et al., 2004).

Mesonaic acid H (**5**) was obtained as white powders ( $[\alpha] +27.3$  ( $c$  0.5, MeOH) with a molecular formula C<sub>30</sub>H<sub>46</sub>O<sub>8</sub> (8 DOU) determined by the HRESIMS ion at  $m/z$  533.3124 [M - H]<sup>-</sup> (calcd. for C<sub>30</sub>H<sub>45</sub>O<sub>8</sub>, 533.3109). Compound **5** was thought to be a urs-12-ene derivative where one methyl doublet ( $\delta_{\text{H}}$  0.98 d,  $J = 6.5$  Hz), seven methyls, one tri-substituted olefinic double bond ( $\delta_{\text{H}}$  5.31 t,  $J = 4.0$  Hz/ $\delta_{\text{C}}$  128.4 and  $\delta_{\text{C}}$  138.0), and three carboxyl groups ( $\delta_{\text{C}}$  174.2, 179.0 and 182.4) were deduced by <sup>1</sup>H- and <sup>13</sup>C-NMR spectra (Tables 1, 2). Except for one secondary hydroxyl group and two carboxyl groups, the overall similarity concerning the chemical shifts of remaining carbons made the chemical skeleton of ursane-type triterpene acid with seven unmodified methyls. Based on HMBC correlations (Figure 2), the secondary OH group was assigned at C-22 by the resonances of H-22 ( $\delta_{\text{H}}$  3.71 dd,  $J = 4.5$  and  $12.0$  Hz)/C-17 ( $\delta_{\text{C}}$  53.5) and carboxyl C-28 ( $\delta_{\text{C}}$  179.0). The HMBC correlations of both CH<sub>3</sub>-23 ( $\delta_{\text{H}}$  1.29 s) and CH<sub>3</sub>-24 ( $\delta_{\text{H}}$  1.28 s) to carboxyl C-3 ( $\delta_{\text{C}}$  182.4), C-4 ( $\delta_{\text{C}}$  46.1), and C-5 ( $\delta_{\text{C}}$  48.4) pointed out that there are two carboxyl groups one at C-3 and the other at C-2. It means that the C-C bond between C-2 and C-3 is broken likely by an oxidative cleavage, and compound **5** has a *secoring* A. The stereochemistry of **5** is identical to regular ursane triterpene acids in which  $\alpha$ -orientation of OH-22 is supported by the NOESY correlations as shown in Figure 3. Added together, compound **5** was determined to be 19 $\alpha$ ,22 $\alpha$ -dihydroxy-2,3-secours-12-ene-28-oic acid.

Compound **6**,  $[\alpha] +21.8$  ( $c$  0.5, MeOH), was isolated as white amorphous powders and had a molecular formula of C<sub>29</sub>H<sub>44</sub>O<sub>5</sub> determined by sodiated quasimolecular ion at  $m/z$  495.3072 [M + Na]<sup>+</sup> (calcd. for C<sub>29</sub>H<sub>44</sub>O<sub>5</sub>Na, 495.3081) in the HRESIMS experiment. The IR, <sup>1</sup>H, and <sup>13</sup>C-NMR spectroscopic data are very similar to compound **4**. Detailed analysis of their data, compound **6** possesses an exocyclic double bond ( $\delta_{\text{H}}$  4.68 brs,

5.01 brs;  $\delta_{\text{C}}$  151.1, 109.3), which replaced a carboxyl group and a singlet methyl in **4**. The complete chemical structure and NMR assignment (Tables 1, 2) were further established and confirmed by 1D and 2D NMR to be identified as 2 $\alpha$ ,3 $\alpha$ ,19 $\alpha$ -trihydroxy-24-norursa-4 (23),12-dien-28-oic acid (Jang et al., 2005).

Compound **7** was collected as an oil sample ( $[\alpha] +9.1$ ,  $c$  0.5 in MeOH) with a molecular formula C<sub>22</sub>H<sub>32</sub>O<sub>5</sub> (on par with 7 DOU) deduced from the HRESIMS ion at  $m/z$  399.2148 [M + Na]<sup>+</sup> (calcd. for C<sub>22</sub>H<sub>32</sub>O<sub>5</sub>Na, 399.2142). According to <sup>13</sup>C-NMR and DEPT spectra (Table 3), the 22 carbons can be divided into three methyls, six methylenes (one oxymethylene at  $\delta_{\text{C}}$  67.7), eight methines [including one oxymethine at  $\delta_{\text{C}}$  69.3 and five sp<sup>2</sup> methines at  $\delta_{\text{C}}$  128.1 (2), 129.0 (2), and 132.7], and five quaternary carbons (two oxygenated ones at  $\delta_{\text{C}}$  72.0 and 74.0, one sp<sup>2</sup> quaternary carbon at  $\delta_{\text{C}}$  130.4, and one ester carbonyl at  $\delta_{\text{C}}$  166.0). In the <sup>1</sup>H-NMR spectrum (Table 3), three methyl singlets ( $\delta_{\text{H}}$  1.02 s, 1.12 s, and 1.19 brs), one oxygenated methylene [ $\delta_{\text{H}}$  3.46 s (2H)] and one oxygenated methine [ $\delta_{\text{H}}$  3.46 s (2H) and 5.18 ddd,  $J = 4.2, 7.8,$  and  $12.0$  Hz] together with the multiple peaks of mono-substituted benzene protons ( $\delta_{\text{H}}$  7.45–7.98) distributed spread from upfield to downfield. Combining the information, compound **7** was reasoned to have a double-ring moiety in addition to a benzene and an ester carbonyl portion. A comprehensive analysis of <sup>1</sup>H–<sup>1</sup>H COSY and HMBC spectra, an eudesmane-type sesquiterpene (Evans et al., 1982) was put forward by incorporating two COSY fragments (H<sub>2</sub>-1/H-2/H<sub>2</sub>-3 and H-5/H<sub>2</sub>-6/H-7/H<sub>2</sub>-8/H<sub>2</sub>-9) and the correlations of HMBC at CH<sub>3</sub>-14/C-1, C-5, C-9, and C-10 and CH<sub>3</sub>-15/C-3, C-4, and C-5. Moreover, the attachments of an *O*-benzoyl (OBz) group and a propane-1,2-diol group were confirmed to be at C-2 and C-7 by the HMBC correlations: H-2, H-2', and H-3' to ester carbonyl C-1'; H<sub>2</sub>-12 and H<sub>3</sub>-13 to C-7 and C-11 (Figure 4A). Concerning the stereochemistry of **7**, it was concluded to be a regular eudesmane-type sesquiterpene with anti-relationships of  $\alpha$ -oriented H-5 and  $\beta$ -oriented CH<sub>3</sub>-14. Furthermore, both the cross peaks of NOESY correlations for H-2/H $\beta$ -3, H-2/CH<sub>3</sub>-14, and H-2/CH<sub>3</sub>-15 suggested the  $\beta$ -orientation of H-2 and CH<sub>3</sub>-14 but  $\alpha$ -orientation of H-7 given H $\alpha$ -3/H-5, and H-5/H-7 (Figure 4B). However, the conformation of C-11 was not unambiguous because it cannot be differentiated directly by the NOESY correlations of H-7/CH<sub>3</sub>-13, H $\alpha$ -8/CH<sub>3</sub>-13, H $\beta$ -8/CH<sub>3</sub>-14, and H $\beta$ -8/H<sub>2</sub>-12. For this reason, the dimolybdenum tetra-acetate [Mo<sub>2</sub>(OAc)<sub>4</sub>]-modified CD analysis was applied to resolve the steric assignment of the acyclic propane-1,2-diol group, a prim, sec-glycol (Frelek et al., 1997). As in many *vic*-glycols with a rigid conformation, one can follow the “helicity rule” to interpret the CD curves, whereby a positive (negative) torsional angle in the (HO)–C–C–(OH) moiety should lead to a positive (negative) Cotton effect of 300 nm. In Figure 4C, a negative CD band at 300 nm is obvious and accompanied by a second Cotton effect of the same sign at around 400 nm corresponding to a negative torsional angle in the (HO)–C–C–(OH) moiety. A Newman projection for the propane-1,2-diol moiety in chelation with Mo<sub>2</sub>(OAc)<sub>4</sub> demonstrated a counterclockwise (a negative torsional angle) relationship from

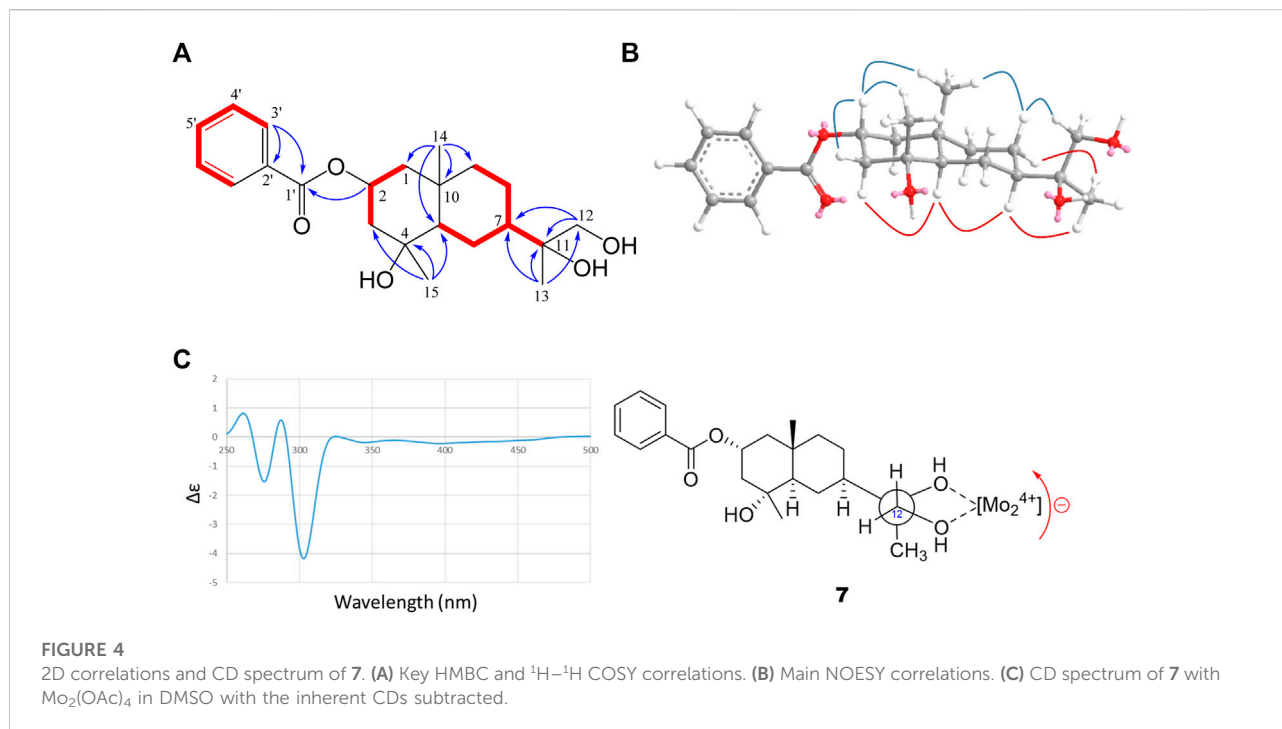


TABLE 4 Anti-NO production activity of compounds 1–7.

Compound	$\text{EC}_{50}$ ( $\mu\text{M}$ ) <sup>a</sup>	Cell viability (%) <sup>b</sup>
<b>1</b>	$20.34 \pm 0.61$	$102.57 \pm 0.29$
<b>2</b>	$21.21 \pm 0.52$	$101.43 \pm 0.14$
<b>3</b>	>30	$103.31 \pm 0.37$
<b>4</b>	>30	$99.41 \pm 0.50$
<b>5</b>	>30	$100.94 \pm 0.42$
<b>6</b>	$20.23 \pm 0.12$	$101.52 \pm 0.16$
<b>7</b>	$12.88 \pm 0.23$	$102.56 \pm 0.32$
Quercetin <sup>c</sup>	$24.12 \pm 0.21$	$100.41 \pm 0.53$

<sup>a</sup>Cells were treated with LPS (1  $\mu\text{g}$ ) in combination with the test compound for 24 h.

<sup>b</sup>Cell viability was measured in the presence of 30  $\mu\text{M}$  compound using the CCK-8 assay.

<sup>c</sup>Quercetin was used as a positive control.

OH-12 to OH-11. Finally, compound **7** was clearly identified as 2-*O*-benzoyl-proximadiol, named mesoeudesmol B.

### 3.2 Effects of compounds 1–7 on RAW264.7 macrophage cell viability and NO production

*M. procumbens* extracts have been shown with pharmacological potentialities for many inflammation-associated disorders (Huang et al., 2012; Huang et al., 2021).

Given the isolated compounds **1**–**7** from *M. procumbens*, we examined these isolates to see whether they similarly exhibit anti-inflammatory activities by using the LPS-induced RAW 264.7 macrophage cell model. As shown in Table 4, mesonaic acids D (**1**) and E (**2**), 2 $\alpha$ ,3 $\alpha$ ,19 $\alpha$ -trihydroxy-24-norursa-4 (23),12-dien-28-oic acid (**6**), and mesoeudesmol B (**7**) show lower  $\text{EC}_{50}$  values than the positive control, quercetin (Li et al., 2016), suggesting that these four compounds possess better anti-inflammatory activity than those previously reported. Among them, mesoeudesmol B (**7**), a proximadiol derivative, displayed the highest inhibition activity on NO production with an  $\text{EC}_{50}$  value of  $12.88 \pm 0.23 \mu\text{M}$  than that of quercetin (an  $\text{EC}_{50}$  value of  $24.12 \pm 0.21 \mu\text{M}$ ). Furthermore, all these seven compounds (at a concentration of 30  $\mu\text{M}$ ) showed an approximate 100% survival rate in cell viability assay, suggesting that they are, in general, safe with no major cytotoxicity (to RAW264.7 cells).

### 3.3 Effects of compound 7 on the protein expression of iNOS and COX-2

To better understand the anti-inflammatory mechanism of compound **7**, we examined two key inflammation-mediated proteins in LPS-induced RAW264.7 cells, iNOS and COX-2 at the protein level (Murakami and Ohgashi, 2007). In terms of the expression level of iNOS and COX-2 shown in Figure 5A, the LPS-treated cells display a higher level as opposed to the non-

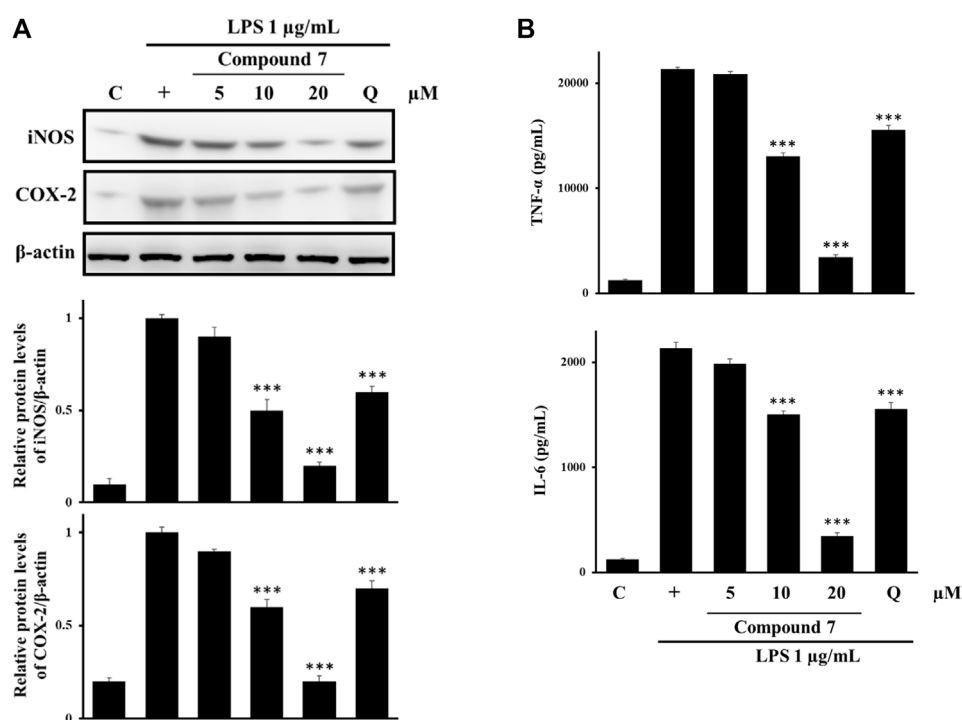


**FIGURE 5** Effects of **7** on the expression of the iNOS and COX-2 proteins and cytokine secretion. RAW 264.7 cells were pretreated with the compounds for 1 h followed by stimulation with LPS (1 μg/ml) for an additional 24 h. **(A)** The expression of iNOS and COX-2 was determined using western blot analysis. The relative levels of iNOS and COX-2 were quantified by normalization to the β-actin levels. **(B)** The levels of TNF-α and IL-6 were measured using ELISA kits. Cells were treated with **7** at a concentration of 5–20 μM. Q: quercetin (25 μM). The data shown here represent the mean values of three independent experiments. \*\*\**p* < 0.001 compared with the group treated with LPS.

treated cells, which show a low expression level. In addition, the protein level of the LPS-induced iNOS and COX-2 is negatively proportional to the addition of mesoeudesmol B (**7**) (5–20 μM) into the LPS-treated cells in a dose-dependent manner. Notably, 10 μM of **7** exhibits the lowest iNOS/COX-2 than 25 μM of quercetin does; moreover, the protein level of iNOS and COX-2 in the LPS-treated cells with the addition of **7** (20 μM) is nothing more than that in the non-treated cells, confirming that sesquiterpene **7** possesses stronger inhibitory activity than quercetin.

### 3.4 Effects of compound **7** on the secretion of cytokines TNF-α and IL-6

Given that TNF-α and IL-6 are major pro-inflammatory cytokines, they were further measured by ELISA in the LPS-stimulated murine macrophages. As shown in **Figure 5B**, it shows a dose-dependent suppression of the LPS-induced secretion of cytokines TNF-α and IL-6 with the addition of compound **7**, which shows a similar trend to that of the LPS-induced expression of iNOS and COX-2. Likewise, 10 μM of **7**

exhibits a lower level of TNF-α and IL-6 than 25 μM of quercetin does; the level of TNF-α and IL-6 in the LPS-treated cells with the addition of **7** (20 μM) is close to the basal one, once again confirming that **7** is a stronger inflammatory inhibitor than quercetin.

## 4 Conclusion

Several lines of evidence have underscored that the phenolics (i.e. kaempferol and caffeic acid), triterpenoids (i.e. oleanolic acid and ursolic acid), and polysaccharides in *M. procumbens* Hemesley are functional ingredients with strong antioxidant and anti-inflammatory properties, thus making Hsian-tsao a superb heat-clearing (Qingre) and detoxifying (Jiedu) herb. Having gone through rigorous and comprehensive interrogations against the literature and chemical databases, the five triterpene acids (**1–5**) and one sesquiterpene (**7**) discovered herein are new chemical entities; mesoeudesmol B (**7**) featuring a proximadiol core structure, in particular, is the first of its kind isolated from the extract of *M. procumbens* Hemesley. Of them, three triterpene acids (**1**, **2**, and **6**)

showed strong anti-inflammatory activities with the EC<sub>50</sub> values of 20.3, 21.1, and 20.2 μM comparable to quercetin (EC<sub>50</sub> values of 24.1 μM) and 15 triterpene acids isolated from our previous study, all presenting strong and promising anti-inflammatory potentials (Huang et al., 2021).

Of them, mesoeudesmol B (7), a 2-OBz proximadiol, outperformed others with an EC<sub>50</sub> value of 12.9 μM 2-fold higher than quercetin in terms of anti-inflammation. Proximol® (cryptomeridiol, a eudesmane sesquiterpenoid) is a well-known Egyptian folk medicine effective as a renal antispasmodic and diuretic agent extracted from the desert weed *Cymbopogon proximus* Stapf (Gramineae) but also from other species, such as *Dysphania graveolens* (Gui et al., 2020) and *Chenopodium vulvariap* (Locksley et al., 1982). This active sesquiterpene is best known for its high antidiabetic activity, whereas the *C. proximus* extracts are more versatile exhibiting multiple bioactivities, including antihypertensive activity and relaxation of the smooth muscle fibers (El-Nezhawy et al., 2014).

We believe that mesoeudesmol B (7) is the dominant agent in *M. procumbens*. The anti-inflammation mechanism of 7 is that it suppresses inflammation-mediated proteins (iNOS and COX-2) and pro-inflammatory cytokines (TNF-α and IL-6), thereby underscoring Hsian-tiao (the grass jelly herb) a superb medicinal herb worth of further studies for advanced pharmacologic applications and biosynthetic diversifications.

## Data availability statement

The datasets presented in this study can be found in online repositories. The names of the repository/repositories and accession number(s) can be found in the article/Supplementary Material.

## Author contributions

H-TH: performing the experiments of the isolation and bioassay and writing the article. I-WL: elucidating the chemical structures and writing the article. G-YL and Y-CS: analyzing and interpreted the bioassay data and writing the article. T-LL: advising on the experiment and revising the

## References

- Azab, A., Nassar, A., and Azab, A. N. (2016). Anti-inflammatory activity of natural products. *Molecules* 21 (10), 1321. doi:10.3390/molecules21101321
- El-Nezhawy, A. O., Maghrabic, I. A., Mohamed, K. M., and Omar, H. A. (2014). *Cymbopogon proximus* extract decreases LNAME-induced hypertension in rats. *Int. J. Pharm. Sci. Rev. Res.* 27 (1), 66–69.
- Evans, F. E., Miller, D. W., Cairns, T., Baddeley, G. V., and Wenkert, E. (1982). Structure analysis of proximadiol (cryptomeridiol) by <sup>13</sup>C NMR spectroscopy. *Phytochemistry* 21 (4), 937–938. doi:10.1016/0031-9422(82)80097-6

article. Y-CL and H-CH: analyzed and interpreted the NMR data. C-CL: conceiving and designing the experiments and editing the article. Y-HK and K-TL: funding acquisition. All authors listed approved it for publication.

## Funding

This research was financially supported by the Ministry of Science and Technology (MOST 107-2320-B-077-003-MY3) and China Medical University (CMU109-MF-02), Republic of China.

## Acknowledgments

The authors sincerely thank all members of the C-CL, Y-HK, and K-TL Laboratories who supported and helped this research.

## Conflict of interest

The authors declare that the research was conducted in the absence of any commercial or financial relationships that could be construed as a potential conflict of interest.

## Publisher's note

All claims expressed in this article are solely those of the authors and do not necessarily represent those of their affiliated organizations, or those of the publisher, the editors, and the reviewers. Any product that may be evaluated in this article, or claim that may be made by its manufacturer, is not guaranteed or endorsed by the publisher.

## Supplementary material

The Supplementary Material for this article can be found online at: <https://www.frontiersin.org/articles/10.3389/fchem.2022.1003356/full#supplementary-material>

- Fan, S. L., Lin, J. A., Chen, S. Y., Lin, J. H., Lin, H. T., Chen, Y. Y., et al. (2021). Effects of hsian-tiao (*Mesona procumbens* hemsl.) extracts and its polysaccharides on the promotion of wound healing under diabetes-like conditions. *Food Funct.* 12 (1), 119–132. doi:10.1039/D0FO02180F

- Feng, T., Ye, R., Zhuang, H., Fang, Z., and Chen, H. (2012). Thermal behavior and gelling interactions of *Mesona blumes* gum and rice starch mixture. *Carbohydr. Polym.* 90 (1), 667–674. doi:10.1016/j.carbpol.2012.05.094

- Frelek, J., Ikekawa, N., Takatsuto, S., and Snatzke, G. (1997). Application of [Mo<sub>2</sub>(OAc)<sub>4</sub>] for determination of absolute configuration of brassinosteroid

vic-diols by circular dichroism. *Chirality* 9 (5-6), 578–582. doi:10.1002/(SICI)1520-636X(1997)9:5/6<578::AID-CHIR27>3.0.CO;2-K

Gui, Y. H., Liu, L., Wu, W., Zhang, Y., Jia, Z. L., Shi, Y. P., et al. (2020). Discovery of nitrogenous sesquiterpene quinone derivatives from sponge *Dysidea septosa* with anti-inflammatory activity *in vivo* zebrafish model. *Bioorg. Chem.* 94, 103435. doi:10.1016/j.bioorg.2019.103435

Huang, G. J., Liao, J. C., Chiu, C. S., Huang, S. S., Lin, T. H., and Deng, J. S. (2012). Anti-inflammatory activities of aqueous extract of *Mesona procumbens* in experimental mice. *J. Sci. Food Agric.* 92 (6), 1186–1193. doi:10.1002/jsfa.4682

Huang, H. T., Liaw, C. C., Chiou, C. T., Kuo, Y. H., and Lee, K. T. (2021). Triterpene acids from *Mesona procumbens* exert anti-inflammatory effects on LPS-stimulated murine macrophages by regulating the MAPK signaling pathway. *J. Agric. Food Chem.* 69 (22), 6271–6280. doi:10.1021/acs.jafc.1c01810

Hung, C. Y., and Yen, G. C. (2002). Antioxidant activity of phenolic compounds isolated from *Mesona procumbens* hemsl. *J. Agric. Food Chem.* 50 (10), 2993–2997. doi:10.1021/jf011454y

Jang, D. S., Kim, J. M., Kim, J. H., and Kim, J. S. (2005). 24-nor-Ursane type triterpenoids from the stems of *Rumex japonicas*. *Chem. Pharm. Bull.* 53 (12), 1594–1596. doi:10.1248/cpb.53.1594

Kashiwada, Y., Wang, H. K., Nagao, T., Kitanaka, S., Yasuda, I., Fujioka, T., et al. (1998). Anti-AIDS agents. 30. Anti-HIV activity of oleanolic acid, pomolic acid, and structurally related triterpenoids. *J. Nat. Prod.* 61 (9), 1090–1095. doi:10.1021/np9800710

Lai, L. S., and Liao, C. L. (2002). Dynamic rheology of structural development in starch/decoloured hsian-tso leaf gum composite systems. *J. Sci. Food Agric.* 82 (10), 1200–1207. doi:10.1002/jsfa.1171

Lai, L. S., Liu, Y. L., and Lin, P. H. (2003). Rheological/textural properties of starch and crude hsian-tso leaf gum mixed systems. *J. Sci. Food Agric.* 83 (10), 1051–1058. doi:10.1002/jsfa.1506

Li, Y., Yao, J., Han, C., Yang, J., Chaudhry, M. T., Wang, S., et al. (2016). Quercetin, inflammation and immunity. *Nutrients* 8 (3), 167. doi:10.3390/nu8030167

Lin, K. H., Shih, M. C., Wang, P., Yu, Y. P., and Lu, C. P. (2018). Effect of different ethanolic concentrations on antioxidant properties and cytoprotective activities of *Platostoma palustre* blume. *Nat. Prod. Res.* 32 (24), 2959–2963. doi:10.1080/14786419.2017.1392952

Liu, X., Shi, B. F., and Yu, B. (2004). Four new dimeric triterpene glucosides from *Sanguisorba officinalis*. *Tetrahedron* 60 (50), 11647–11654. doi:10.1016/j.tet.2004.09.045

Locksley, H. D., Fayez, M. B. E., Radwan, A. S., Chari, V. M., Cordell, G. A., and Wagner, H. (1982). Constituents of local plants. XXV, constitution of the antispasmodic principle of *Cymbopogon proximus*. *Planta Med.* 45 (5), 20–22. doi:10.1055/s-2007-971233

Murakami, A., and Ohigashi, H. (2007). Targeting NOX, INOS and COX-2 in inflammatory cells: Chemoprevention using food phytochemicals. *Int. J. Cancer* 121 (11), 2357–2363. doi:10.1002/ijc.23161

Shyu, M. H., Kao, T. C., and Yen, G. C. (2008). Hsian-tso (*Mesona procumbens* hemsl.) prevents against rat liver fibrosis induced by CCl<sub>4</sub> via inhibition of hepatic stellate cells activation. *Food Chem. Toxicol.* 46 (12), 3707–3713. doi:10.1016/j.fct.2008.09.051

Singh, N., Baby, D., Rajguru, J. P., Patil, P. B., Thakkannavar, S. S., and Pujari, V. B. (2019). Inflammation and cancer. *Ann. Afr. Med.* 18 (3), 121–126. doi:10.4103/aam.aam\_56\_18

Yang, M., Xu, Z. P., Xu, C. J., Meng, J., Ding, G. Q., Zhang, X. M., et al. (2008). Renal protective activity of hsian-tso extracts in diabetic rats. *Biomed. Environ. Sci.* 21 (3), 222–227. doi:10.1016/S0895-3988(08)60033-1

Yeh, C. T., Huang, W. H., and Yen, G. C. (2009). Antihypertensive effects of hsian-tso and its active compound in spontaneously hypertensive rats. *J. Nutr. Biochem.* 20 (11), 866–875. doi:10.1016/j.jnutbio.2008.07.015

Yeh, Y. H., Liang, C. Y., Chen, M. L., Tsai, F. M., Lin, Y. Y., Lee, M. C., et al. (2019). Apoptotic effects of hsian-tso (*Mesona procumbens* Hemsley) on hepatic stellate cells mediated by reactive oxygen species and ERK, JNK, and caspase-3 pathways. *Food Sci. Nutr.* 7 (5), 1891–1898. doi:10.1002/fsn3.1046

Yen, G. C., Duh, P. D., and Hung, Y. L. (2001). Contributions of major components to the antimutagenic effect of hsian-tso (*Mesona procumbens* hemsl.). *J. Agric. Food Chem.* 49 (10), 5000–5004. doi:10.1021/jf0103929

Yen, G. C., and Hung, C. Y. (2000). Effects of alkaline and heat treatment on antioxidative activity and total phenolics of extracts from hsian-tso (*Mesona procumbens* hemsl.). *Food Res. Int.* 33 (6), 487–492. doi:10.1016/S0963-9969(00)00073-9

Yen, G. C., Hung, Y. L., and Hsieh, C. L. (2000). Protective effect of extracts of *Mesona procumbens* hemsl. On DNA damage in human lymphocytes exposed to hydrogen peroxide and UV irradiation. *Food Chem. Toxicol.* 38 (9), 747–754. doi:10.1016/S0278-6915(00)00069-7

Zhuang, H., Feng, T., Xie, Z., Toure, A., Xu, X., Jin, Z., et al. (2010). Effect of *Mesona blumes* gum on physicochemical and sensory characteristics of rice extrudates. *Int. J. Food Sci. Technol.* 45 (11), 2415–2424. doi:10.1111/j.1365-2621.2010.02426.x